

A multi-purpose, multi-frequency Shuttlecock Antenna for CubeSats

R. Lehmensiek

Department of Electrical Engineering, Cape Peninsula University of Technology
Bellville, South Africa, lehmsk@ieee.org

1. Introduction

CubeSats [1] may use radio communication systems in various frequency bands [2]. Due to the space constraints on a CubeSat and because the system's power availability needs to be maximised by means of maximising the solar panel surface area, the number of possible payload devices and antennas on the satellite, and the size thereof, is limited. Thus there is merit in using a multi-frequency single-port antenna which can transmit and receive on several frequencies using a single antenna structure. Furthermore, if this antenna structure also forms part of a passive aerodynamic attitude stabilisation system, it provides for a very attractive solution.

CubeSats typically have little or no attitude control because the traditional attitude stabilisation systems used on larger satellites, i.e. sensors and actuators, are impractical due to their size, weight and power budget requirements. However, for low earth orbiting satellites at altitudes below 500 km it is feasible to use aerodynamic drag torques together with a damping mechanism for rough attitude stabilisation. In [3] thin metallic strips or feathers (due to the resemblance to a badminton shuttlecock) that deploy after launch from the rear of the satellite were used. These feathers stabilise the satellite in pitch and yaw due to the passive aerodynamic drag torques. The damping was done using an active magnetic torque control system.

In this paper a multi-purpose four-feathered satellite antenna (similar to that in [3]) that is used both for passive attitude stabilisation and as a multi-frequency antenna is investigated for a 3U CubeSat. The four feathers made from thin metallic strips are connected to a passive impedance matching network at the rear of the satellite. The matching network combines the four feathers and impedance matches to a single port 50 ohm coaxial connector. The antenna was designed to radiate at the amateur satellite communication frequencies: 435 – 438 MHz (UHF) and 1260 – 1270 MHz (L-band). Bandstop filters are cut into the metal strips to suppress currents along the length of the wire to simulate shorter or longer wire lengths at different frequencies, thus creating a multi-frequency antenna. Full-wave electromagnetic analyses of the complete antenna structure on a 3U CubeSat are presented.

2. Antenna Design

Assuming a pitch and yaw stabilised satellite, the antenna requirement is an omnidirectional antenna pattern (with the null orientated along the roll axis) so that a communications link between the satellite and the ground station for any roll angle is maintained. The antenna is required to maximise the communication time when the satellite is above the horizon. For the CubeSat system under consideration a minimum of -10 dBi antenna gain is required when the antenna is directly overhead the ground station at an altitude of 600 km, i.e. $\theta_a = 0^\circ$, and the required minimum antenna gain increases as θ_a increases. The coordinate system and the geometric quantities used are defined in Figure 1. Note that the satellite height above ground is typically required to be well below 600 km so that the earth's atmosphere can provide enough drag torque for the passive aerodynamic system to work. Thus, an altitude of 600 km as used here can be considered a worst case scenario. For an altitude of 400 km the free space loss decreases by about 3.5 dB (at $\theta_a = 0^\circ$).

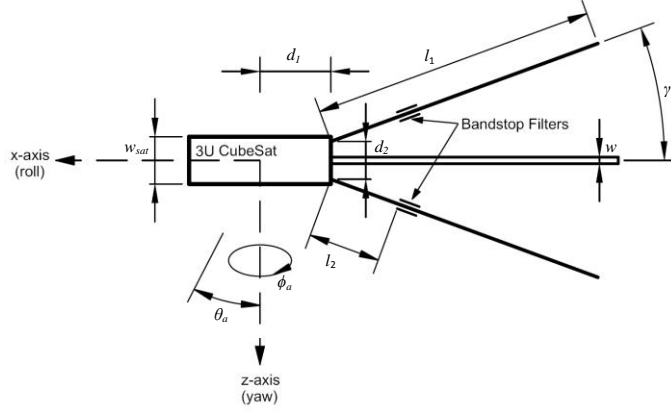


Figure 1: Geometry of the four-feathered multi-frequency antenna structure on a 3U CubeSat. The y-axis (pitch) points into the paper.

2.1 Antenna Coverage Efficiency

An antenna coverage efficiency, η_a , was defined as follows according to the solid angle that the designed antenna pattern subtends relative to the maximum possible solid angle that an ideal (maximum coverage to the horizon) antenna, would subtend:

$$\eta_a = \frac{\int_{\phi_a=0}^{\phi_a=2\pi} \int_{\theta_a=0}^{\theta_a=\theta_a(\phi_a)} u(\theta_a, \phi_a) \sin \theta_a d\theta_a d\phi_a}{\int_{\phi_a=0}^{\phi_a=2\pi} \int_{\theta_a=0}^{\theta_a=\theta_o} \sin \theta_a d\theta_a d\phi_a}, \quad (1)$$

where θ_a is the antenna elevation angle, ϕ_a is the antenna azimuth angle (as defined in Figure 1) and $u(\theta_a, \phi_a)$ is equal to 1 if the antenna gain is bigger than the required minimum gain for radio communication and zero otherwise. The elevation angle, θ_o , is the antenna elevation angle to the ground station when the satellite is at the horizon relative to the ground station. For a satellite altitude of 600 km, θ_o is about 66° . This efficiency definition has similarity to the antenna gain definition [4].

2.2 First Order Investigation

A model of the 3U CubeSat and antenna structure, similar to that shown in Figure 1 (without the bandstop filter), was analysed with the full wave commercially available computational electromagnetic code FEKO [5] for various feather lengths, l_1 , and feather angles, γ . As the feather width, w , will have little influence on the radiation pattern, it was not varied and chosen as 15 mm. The distance d_2 was chosen as 80 mm to maximise the torque (see Section 3) and to allow space for implementation of a deployment mechanism. In these analyses a perfectly electrically conductive right square cylinder was assumed as the satellite body and perfectly electric conductive flat rectangular strips as the feathers.

For the UHF frequency there are two maxima roughly at $l_1 = 630$ mm, $\gamma = 12^\circ$, and $l_1 = 400$ mm, $\gamma = 41^\circ$ with an antenna coverage efficiency of $\eta_a = 94.0\%$ and $\eta_a = 93.7\%$ respectively. The antenna coverage efficiency at these maxima is only $\eta_a = 79.2\%$ and $\eta_a = 74.9\%$ at the L-band frequency and, as expected, improves for shorter feather lengths. The maxima at the L-band frequency for an antenna coverage efficiency above 90% are roughly at $l_1 = 250$ mm, $\gamma = 13^\circ$, $l_1 = 130$ mm, $\gamma = 20^\circ$ and $l_1 = 220$ mm, $\gamma = 45^\circ$, with efficiencies $\eta_a = 93.9\%$, $\eta_a = 93.0\%$ and $\eta_a = 91.3\%$ respectively.

The analyses also showed that the antenna coverage efficiency is not sensitive to the parameters l_1 and γ especially at the lower frequency, thus allowing a wide choice of parameters for the passive aerodynamic system. As the feather angle γ has to be the same at both frequencies, a compromise has to be made and an angle chosen that is optimal for both frequencies. In the next section the bandstop filter is described and then the maxima above are used as starting values for a full optimisation of the relevant parameters to find an optimal solution.

2.3 Bandstop Filter

In order for the metallic strips to appear shorter at the higher frequency, bandstop filters are added at suitable locations along the length of the strip. These parallel-tuned resonant circuits provide a high impedance to the current at the higher frequency, but are reasonably transparent at the lower frequency. This concept was used in the early times of radio for low frequency band antennas [6]. The bandstop filter can be realised by a shunt LC resonant circuit which is resonant at the higher frequency. Several filter configurations are possible. The configuration used in this paper was an inductor realised by two thin lines on the edge of the metallic strip and a capacitor realised by an interdigital capacitor in the middle of the strip.

2.3 Full Optimisation

The bandstop filter is not perfect and affects both the antenna radiation pattern and the antenna impedance. To compensate for these effects an optimisation technique was used to determine the antenna parameters that have the best performance at both frequencies starting with the maxima as determined in Section 2.1. A solution with the best electromagnetic performance that also provides reasonable pitch and yaw stiffness together with low drag is shown in Figure 2 and Figure 3. The resultant coverage efficiency is 93.7 % at both frequencies and $l_1 = 629.3$ mm, $\gamma = 12.8^\circ$ and $l_2 = 238.4$ mm.

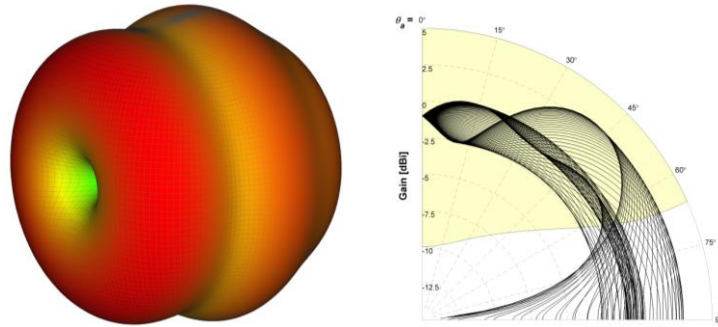


Figure 2: Predicted 3D radiation pattern at 436.5 MHz and the corresponding pattern cuts with ϕ_a in 2° increments. The shaded area depicts the required antenna coverage for a satellite at 600 km.

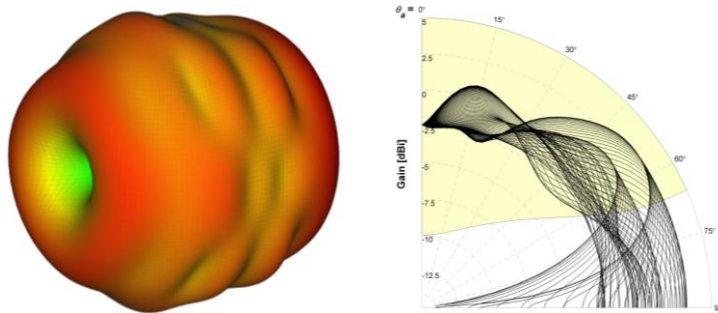


Figure 3: Predicted 3D radiation pattern at 1265 MHz and the corresponding pattern cuts with ϕ_a in 2° increments. The shaded area depicts the required antenna coverage for a satellite at 600 km.

5. Impedance Matching Network

The proposed topology of the matching network for each feather consists of two transmission lines with a short-circuited stub in between them. The shorted transmission line offers a path to convey electrostatic discharges. The physical configuration of the matching network using microstrip lines on RO4003 substrate is shown in Figure 4. The resultant reflection coefficient, after optimisation, is shown in Figure 5. The predicted reflection coefficient is well below -30 dB in the UHF band and below -26 dB at the L-band frequencies.

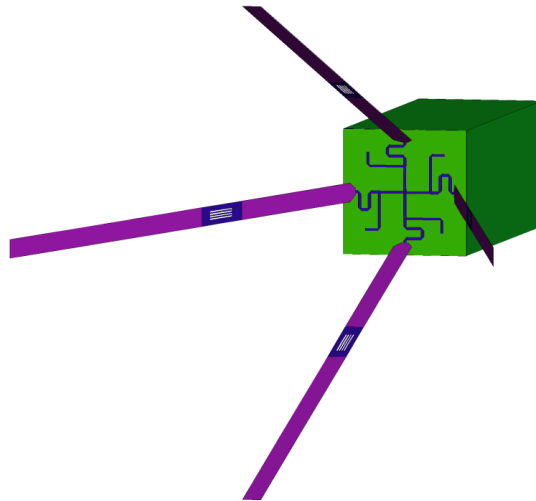


Figure 4: FEKO model of the 3U CubeSat, impedance matching network and the four feathery antennas with band-stop filters.

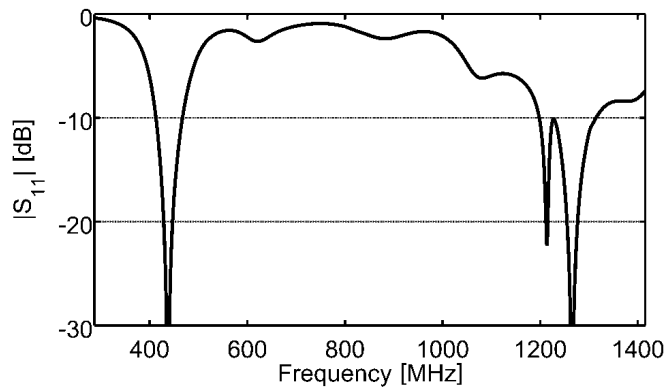


Figure 5: Predicted antenna reflection coefficient.

Acknowledgments

The author acknowledges the French South African Institute of Technology (F'SATI) and the National Research Foundation (NRF) of South Africa for their financial support.

References

- [1] H. Heidt, J. Puig-Suari, A. S. Moore, S. Nakasuka, R. J. Twiggs, "CubeSat: A new generation of picosatellite for education and industry low-cost space experimentation," Proc. 14th Annual USU Small Satellites Conference, paper SSC00-V-5, 2000.
- [2] S. Gao, K. Clark, M. Unwin, J. Zackrisson, W. A. Shiroma, J. M. Akagi, K. Maynard, P. Garner, L. Boccia, G. Amendola, G. Massa, C. Underwood, M. Brenchley, M. Pointer, M. N. Sweeting, "Antennas for modern small satellites", IEEE Antennas & Propagation Mag., vol. 51, no. 4, pp. 40-56, Aug. 2009.
- [3] M. L. Psiaki, "Nanosatellite attitude stabilization using passive aerodynamics and active magnetic torquing", *Journal of Guidance, Control, and Dynamics*, vol. 27, no. 3, May-Jun. 2004.
- [4] C. A. Balanis, *Antenna Theory, Analysis and Design*, 3rd edition, Wiley, 2005.
- [5] EM Software & Systems – S.A. (Pty) Ltd, Stellenbosch, South Africa, FEKO, Suite 5.5, <http://www.feko.info>.
- [6] R. E. Collin, *Antennas and Radiowave Propagation*, McGraw-Hill, 1985.